Electronic Supplementary Information

Rapid synthesis of magnetic metal-organic framework nanocomposites for highly specific separation of histidine-rich proteins

Jiangnan Zheng, Zian Lin, Guo Lin, Huanghao Yang, and Lan Zhang**

Ministry of Education Key Laboratory of Analysis and Detection for Food Safety, Fujian Provincial Key Laboratory of Analysis and Detection Technology for Food Safety, College of Chemistry, Fuzhou University, Fuzhou, Fujian, 350108, China

- First corresponding author: **Zian Lin;**
- Second corresponding author: **Lan Zhang**
- Postal address: **College of Chemistry, Fuzhou University, Fuzhou, Fujian, 350108, China**
- Fax: **86-591-22866135**
- E-mail: **zianlin@fzu.edu.cn (Z.A. Lin); zlan@fzu.edu.cn (L. Zhang);**

Digestion of protein samples

The digestion of protein and human serum was performed according to the conventional procedures. For mass spectrometry (MS) analysis, the adsorbed proteins on Fe_3O_4@ZIF-8 were eluted by 0.1 % formic acid (FA) and neutralized by ammonium hydroxide. Then the eluate was diluted to 1.0 mL by 50 mM ammonium bicarbonate and denatured in a 95 ºC water bath for 5 min. The solution was reduced in 5 mM DTT for 1h at 56 ºC. When cooled to room temperature, cysteines were alkylated in the dark in 10 mM IAA for 1h at room temperature. Then the solution was incubated at 37 ºC for 24 h after adding 200 μg TPCK-trypsin. The digestion of 100-fold human blood sample was the same as the above procedure.

MS analysis and database searching.

MS Detection was performed using an Agilent 1200 series LC system coupled to an Agilent 6520 Q-TOF mass spectrometer (Agilent Technologies, USA). All samples were separated by Agilent Poroshell 120 EC-C18 column (2.7 μm, 50 mm ×3.0 mm). A binary gradient was delivered at 0.3 mL/min using (A) 0.1% formic acid in water and (B) 0.1% formic acid in ACN. Samples were eluted with 3 to 10% B (0–3 min); 10 to 40% B (3–23 min); 40–80% B (20–25 min); 80% B (25–27 min). The drying gas temperature was set at 350°C with a flow rate of 10 L/min. The sample injection volume was 10 μL. The voltage set for the MS capillary was 4 kV and the fragmentor was set to 175 V. Scanning mass range was from m/z 100 to 3000 at an acquisition rate of 3 spectra per second in the auto MS/MS mode. For MS/MS experiments, the collision energy was set to according to the equation:

$$\mathrm{CE\ (V)} = \frac{\left(\frac{m}{z}\right)}{100(Da)}k + b \qquad (1)$$

where *k* is the slope and *b* is the y-intercept of the equation (both of which can be adjusted by the users), *m/z* is the mass-to-charge ratio of the precursor ion. For divalent ions, k and b were set to 3.1 and 1.0, respectively. For trivalent or greater valence ions, k and b were set to 3.6 and 4.8, respectively. The preferred charge states were set at 2, 3, >3 and unknown.

Data analysis was performed on Agilent Mass Hunter. The LC-MS/MS raw data were searched with Spectrum Mill version A.03.03 against a database (target database of *SwissProt.human*) using a precursor mass tolerance of ±20 ppm and a monoisotopic product mass tolerance of ±50 ppm. Trypsin restriction was set with two missed cleavages. Carboxymethylation was set as the static modification; acetylation**,** cysteine sulfoxide, oxidized methionine and serine phosphorylation were set as the variable modifications.

Analysis of surface-exposed His residues of proteins

The number of surface-exposed His residues of proteins were approximated using GETAREA 1.1 software[1] based on the protein crystal structure data from Protein Data Bank (PDB).[2] A probe radius of 1.4 Å, representing the Van der Waals sphere of water, was used. The ratio of side-chain surface area to "random coil" value per residue were listed in Table S1. The "random coil" value of a residue X is the average water-accessible surface area of X in the tripeptide Gly-X-Gly in an ensemble of 30 random conformations. Residues are likely to be water exposed if the ratio value exceeds 30%.

In the zinc (II)-histidine interaction, two endocyclic nitrogen atoms in His, *i.e.* ND1 and NE2 can coordinate with zinc ion. Thus, the extent of ND1 or NE2 atom's surface accessibility would be a critical factor to investigate the interaction of Fe_3O_4@ZIF-8 and His-rich proteins. The area values

of ND1 and NE2 atoms in proteins are also listed in Table S1. ND1 or NE2 atom is regarded as surface-exposed if the surface area exceeds 10 Å^2. In addition, the ND1 and NE2 of a His imidazole ring have pK_as of 6.0 for the first ring nitrogen ionization and 14.4 for the second ionization.[3] Therefore, heme-binding His residues of heme proteins (*e.g.* BHb, Mb, Cyt C, HRP) are unlikely to bind another metal ion at neutral pH condition.

Table S1-1 His residues of BHb (2QSS)

Residue	Subunit	Position	Ratio (%)	Area/Energy		Description
				ND1	NE2	
HIS	Alpha (chain A)	20	67	5.71	18.62	Surface-exposed
HIS	Alpha (chain A)	45	98.3	6.31	18.61	Surface-exposed
HIS	Alpha (chain A)	50	73.1	0.07	0	Inner
HIS	Alpha (chain A)	58	27.4	1.39	5.32	Heme-binding
HIS	Alpha (chain A)	72	47	0	18.61	Surface-exposed
HIS	Alpha (chain A)	87	24.8	0	17.21	Heme-binding
HIS	Alpha (chain A)	89	67.7	5.38	18.59	Surface-exposed
HIS	Alpha (chain A)	103	7.6	2.56	0	Inner
HIS	Alpha (chain A)	112	31.1	10.02	0.29	Surface-exposed
HIS	Alpha (chain A)	122	0.4	0	1.04	Inner
HIS	Beta (chain B)	62	42.9	2.86	13.95	Heme-binding
HIS	Beta (chain B)	76	51.7	12.55	9.76	Surface-exposed
HIS	Beta (chain B)	91	28.9	0	18.03	Heme-binding
HIS	Beta (chain B)	96	33.3	1.66	12.09	Surface-exposed
HIS	Beta (chain B)	142	62.6	4.75	18.64	Surface-exposed
HIS	Beta (chain B)	145	50.2	4.2	0.09	Inner
HIS	Alpha (chain C)	20	57.6	1.32	18.6	Surface-exposed
HIS	Alpha (chain C)	45	65.3	10.38	5.51	Surface-exposed
HIS	Alpha (chain C)	50	72.2	0.13	0	Inner
HIS	Alpha (chain C)	58	26.5	2.38	4.52	Heme-binding
HIS	Alpha (chain C)	72	50.4	0	18.63	Surface-exposed
HIS	Alpha (chain C)	87	25.4	0	16.63	Heme-binding
HIS	Alpha (chain C)	89	38	0	13.98	Surface-exposed
HIS	Alpha (chain C)	103	7.9	2.5	0	Inner

HIS	Alpha (chain C)	112	29.4	10.67	0.01	Inner
HIS	Alpha (chain C)	122	0.5	0	1.19	Inner
HIS	Beta (chain D)	62	39	10.5	3.71	Heme-binding
HIS	Beta (chain D)	76	51.4	11.98	8.41	Surface-exposed
HIS	Beta (chain D)	91	27.2	0	17.01	Heme-binding
HIS	Beta (chain D)	96	38.2	2.1	13	Surface-exposed
HIS	Beta (chain D)	142	41.2	7.84	10.87	Surface-exposed
HIS	Beta (chain D)	145	44.6	5.46	3.22	Inner

Table S1-2 His residues of Mb (1YMB)

Residue	Position	Ratio (%)	Area/Energy		Description
			ND1	NE2	
HIS	24	3.5	0	0	Inner
HIS	36	31.3	4.65	10.18	Surface-exposed
HIS	48	63	4.21	8.45	Inner
HIS	64	26.4	4.43	2.44	Heme-binding
HIS	81	88.9	8.28	19.69	Surface-exposed
HIS	82	3.5	1.45	0.86	Inner
HIS	93	30.1	0	17.51	Heme-binding
HIS	97	43.6	11.43	10.35	Surface-exposed
HIS	113	50.2	9.7	12.05	Surface-exposed
HIS	116	43.8	9.6	0.43	Inner
HIS	119	15.4	5.84	0	Inner

Table S1-3 His residues of HSA dimer (1AO6)

Residue	Subunit	Position	Ratio (%)	Area/Energy		Description
				ND1	NE2	
HIS	A	9	50.4	0.50	11.16	Surface-exposed
HIS	A	39	0	0.00	0.01	Inner
HIS	A	67	18.9	1.99	0.00	Inner
HIS	A	105	24.5	0.00	6.59	Inner
HIS	A	128	52.2	7.65	6.99	Surface-exposed
HIS	A	146	26.9	4.23	12.08	Inner

HIS	A	242	2.7	0.00	1.87	Inner
HIS	A	247	45.4	1.97	8.94	Inner
HIS	A	288	23.4	0.00	14.76	Inner
HIS	A	338	30.5	0.23	11.36	Inner
HIS	A	367	50.6	7.35	0.32	Inner
HIS	A	440	30.2	1.10	6.74	Inner
HIS	A	464	2.6	0.83	0.05	Inner
HIS	A	510	74.7	12.52	16.13	Surface-exposed
HIS	A	535	12.9	0.00	0.78	Inner
HIS	B	9	46.5	0.69	10.21	Surface-exposed
HIS	B	39	0	0.00	0.00	Inner
HIS	B	67	21.9	2.29	0.00	Inner
HIS	B	105	15.7	4.88	0.42	Inner
HIS	B	128	52.3	5.72	9.00	Surface-exposed
HIS	B	146	26.9	2.86	11.10	Inner
HIS	B	242	4.4	0.00	4.37	Inner
HIS	B	247	36.6	0.14	6.21	Inner
HIS	B	288	27.6	0.70	13.88	Inner
HIS	B	338	31.1	0.05	12.91	Inner
HIS	B	367	49.8	9.29	1.56	Partly surface-exposed
HIS	B	440	30.6	1.97	3.09	Inner
HIS	B	464	3.7	1.27	0.00	Inner
HIS	B	510	66.8	1.31	16.58	Surface-exposed
HIS	B	535	9.9	0.00	0.35	Inner

Table S1-4 His residues of BSA dimer (3V03)

Residue	Subunit	Position	Ratio (%)	Area/Energy		Description
				ND1	NE2	
HIS	A	3	11.5	---	---	Inner
HIS	A	9	40.2	3.06	4.37	Inner
HIS	A	18	19.4	0.00	6.87	Inner
HIS	A	39	0.1	0.00	0	Inner
HIS	A	59	48.2	0.00	17.68	Surface-exposed
HIS	A	67	26.1	1.53	4.06	Inner
HIS	A	105	29.9	0.00	3.72	Inner

HIS	A	145	19.2	3.99	2.78	Inner
HIS	A	241	2.8	0.00	2.02	Inner
HIS	A	246	51.7	10.35	8.2	Surface-exposed
HIS	A	287	15.4	0.46	6.76	Inner
HIS	A	337	34	0.00	12.74	Inner
HIS	B	366	26	---	---	Inner
HIS	B	378	34	---	---	Inner
HIS	A	463	2.5	2.38	0	Inner
HIS	A	509	83.4	14.81	14.99	Surface-exposed
HIS	A	534	30.2	0.00	12.35	Inner
HIS	B	3	70	0.32	18.62	Surface-exposed
HIS	B	9	39	3.33	4.06	Inner
HIS	B	18	20.3	0.00	7.59	Inner
HIS	B	39	0.1	0.00	0	Inner
HIS	B	59	48.6	0.00	17.42	Surface-exposed
HIS	B	67	26.7	1.87	4.99	Inner
HIS	B	105	29	0.00	3.72	Inner
HIS	B	145	19.2	3.92	3.13	Inner
HIS	B	241	3.3	0.00	2.27	Inner
HIS	B	246	44.9	11.47	5.67	Surface-exposed
HIS	B	287	15.6	0.65	6.64	Inner
HIS	B	337	34.1	0.00	12.72	Inner
HIS	B	366	44.7	9.09	0.07	Inner
HIS	B	378	58.5	5.50	5.42	Inner
HIS	B	463	2.9	2.41	0	Inner
HIS	B	509	84	13.98	14.25	Surface-exposed
HIS	B	534	29.9	0.00	13.14	Inner

Table S1-5. His residues of Cyt C (1HRC)

Residue	Position	Ratio (%)	Area/Energy		Description
			ND1	NE2	
HIS	18	13.5	0.00	3.11	Heme-binding
HIS	26	25.5	0.00	0.85	Inner
HIS	33	17.5	0.00	3.99	Inner

Table S1-6 His residues of Lyz (1LYZ)

Residue	Position	Ratio (%)	Area/Energy		Description
			ND1	NE2	
HIS	15	21.8	0.00	3.45	Inner

Table S1-7 His residues of HRP (1HCH)

Residue	Position	Ratio (%)	Area/Energy		Description
			ND1	NE2	
HIS	40	0.5	0.10	0.67	Inner
HIS	42	3.9	0.20	4.36	Heme-binding
HIS	170	34.9	0.00	16.41	Heme-binding

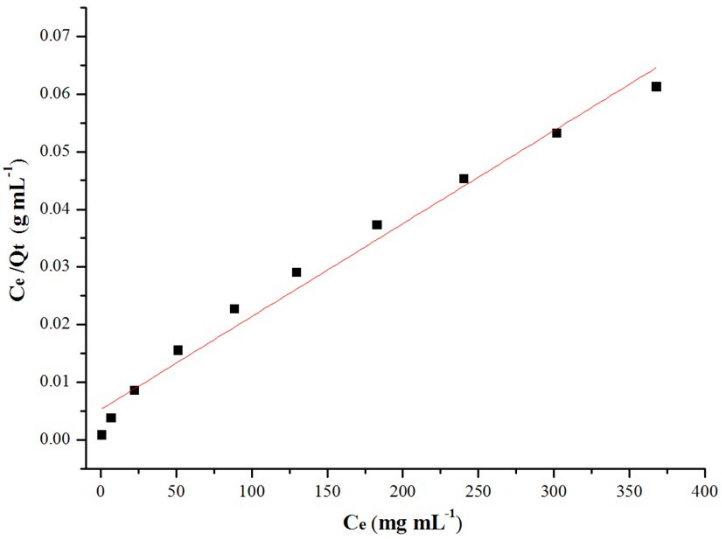

Fig. S1-1 Fitting of the adsorption isotherm of BHb on the Fe_3O_4@ZIF-8 by using the Langmuir model.

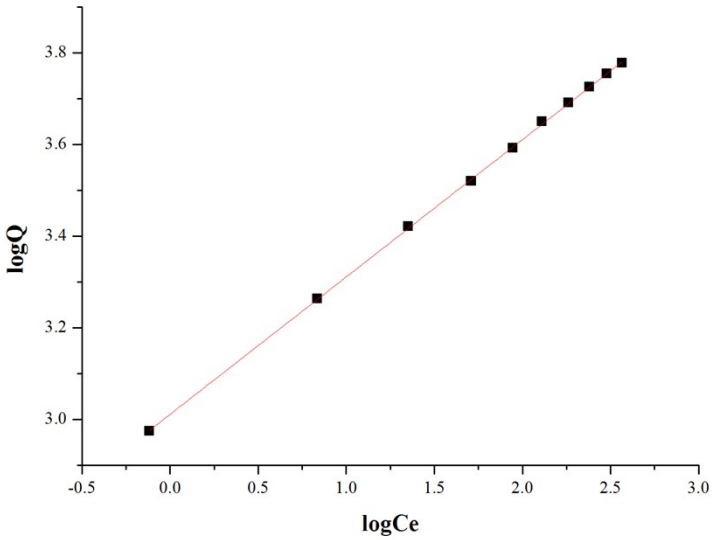

Fig. S1-2 Fitting of the adsorption isotherm of BHb on the Fe_3O_4@ZIF-8 by using the Freundlich model.

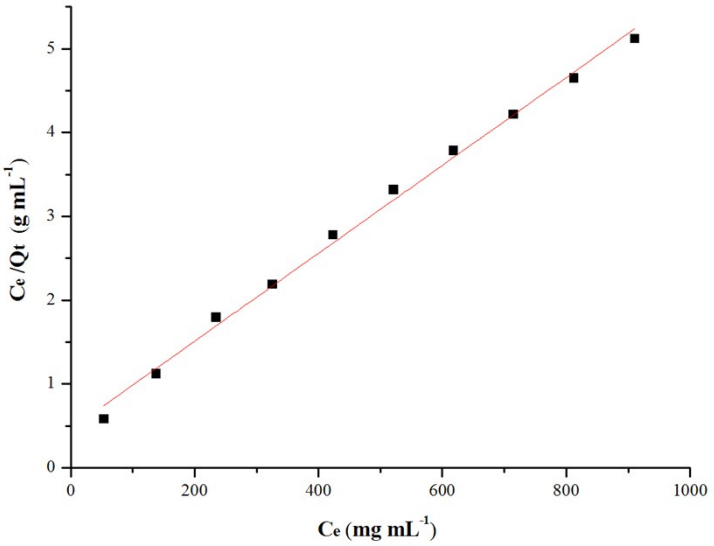

100

101 **Fig. S1-3** Fitting of the adsorption isotherm of Mb on the Fe_3O_4@ZIF-8 by using the Langmuir

102 model.

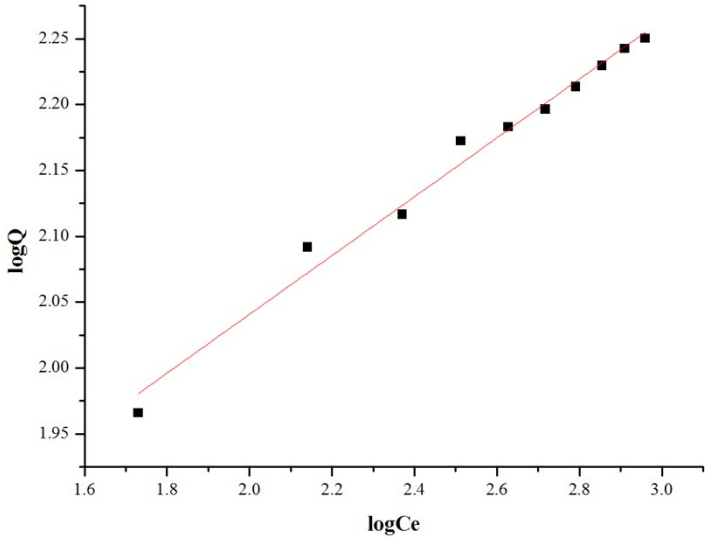

103

104 **Fig. S1-4** Fitting of the adsorption isotherm of Mb on the Fe_3O_4@ZIF-8 by using the Freundlich

105 model.

106

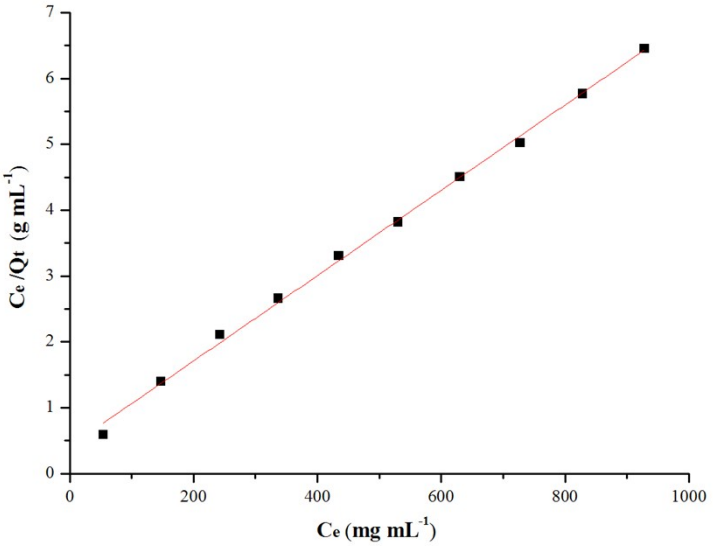

107

108 **Fig. S1-5** Fitting of the adsorption isotherm of HSA on the Fe_3O_4@ZIF-8 by using the Langmuir

109 model.

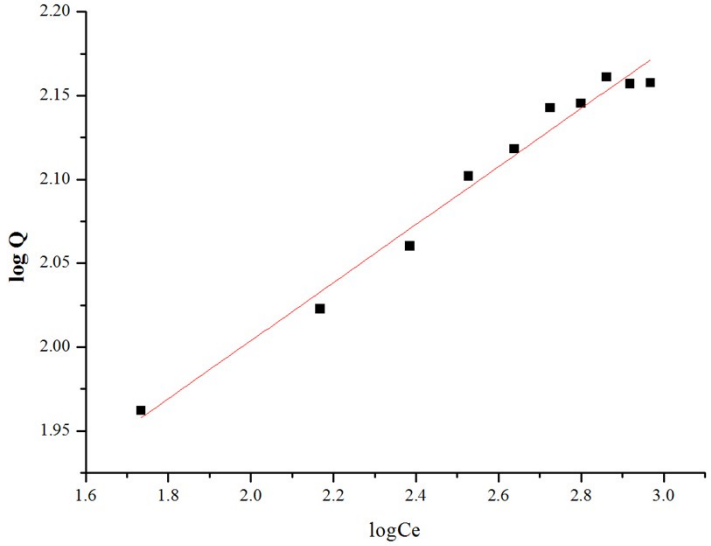

110

111 **Fig. S1-6** Fitting of the adsorption isotherm of HSA on the Fe_3O_4@ZIF-8 by using the Freundlich

112 model.

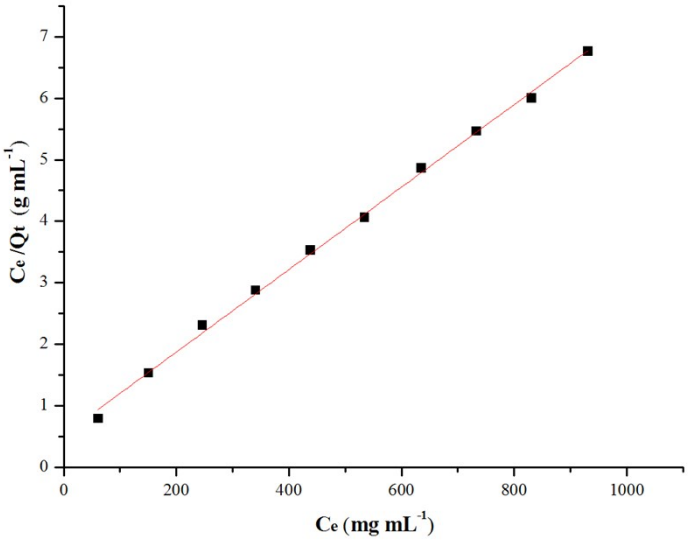

113

114 **Fig. S1-7** Fitting of the adsorption isotherm of BSA on the Fe_3O_4@ZIF-8 by using the Langmuir

115 model. The fitted parameters are summarized in Table S1.

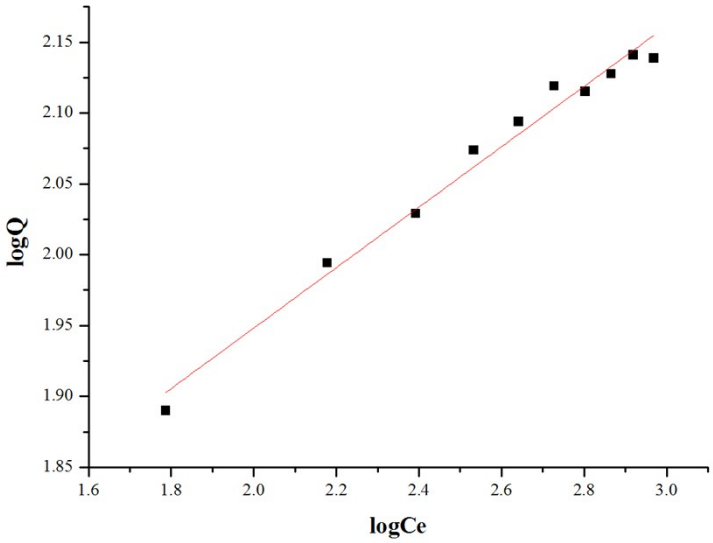

116

117 **Fig. S1-8** Fitting of the adsorption isotherm of BSA on the Fe_3O_4@ZIF-8 by using the Freundlich

118 model.

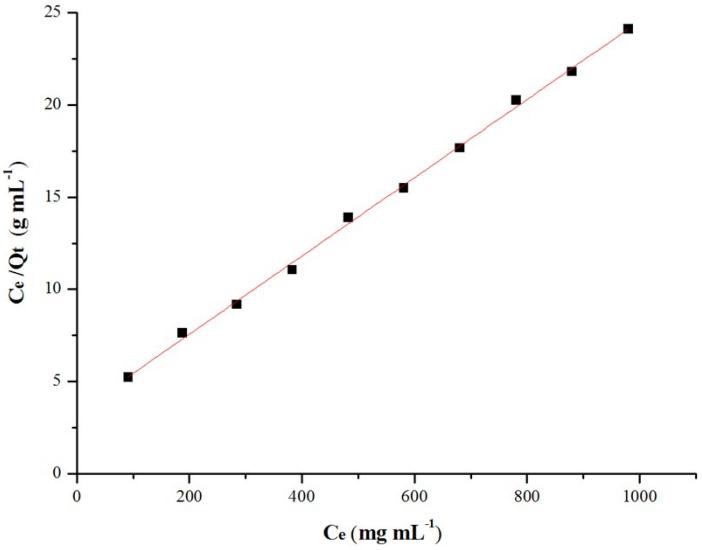

120

121 **Fig. S1-9** Fitting of the adsorption isotherm of Lyz on the Fe_3O_4@ZIF-8 by using the Langmuir

122 model.

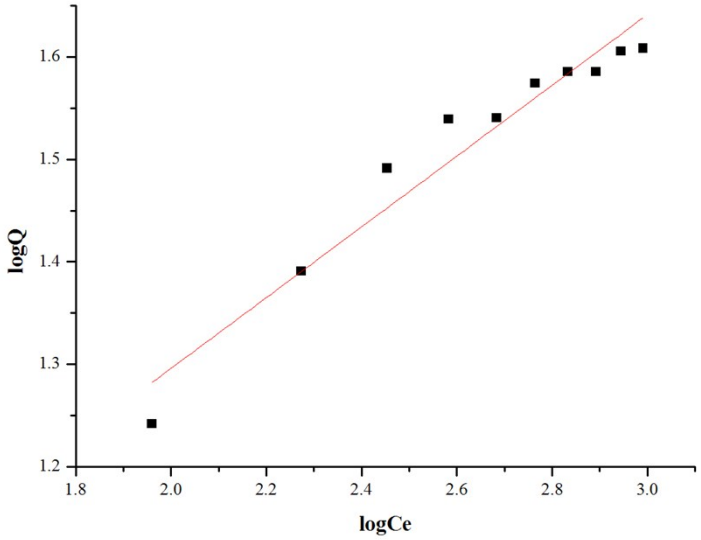

123

124 **Fig. S1-10** Fitting of the adsorption isotherm of Lyz on the Fe_3O_4@ZIF-8 by using the Freundlich

125 model.

126

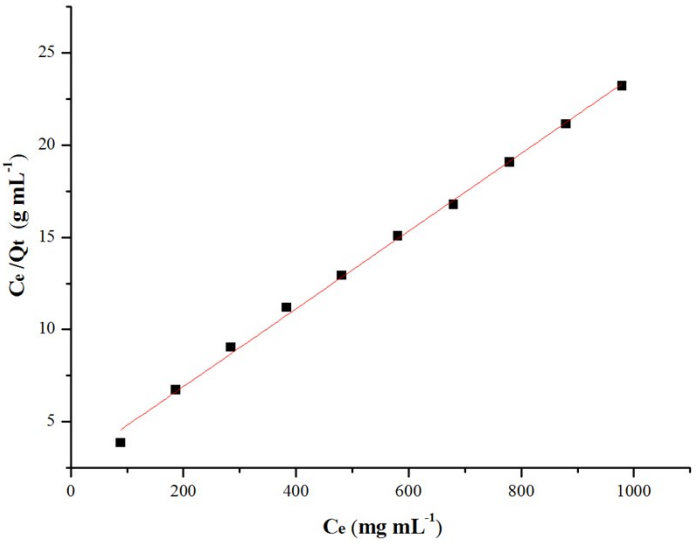

127

128 **Fig. S1-11** Fitting of the adsorption isotherm of CytC on the Fe_3O_4@ZIF-8 by using the Langmuir

129 model.

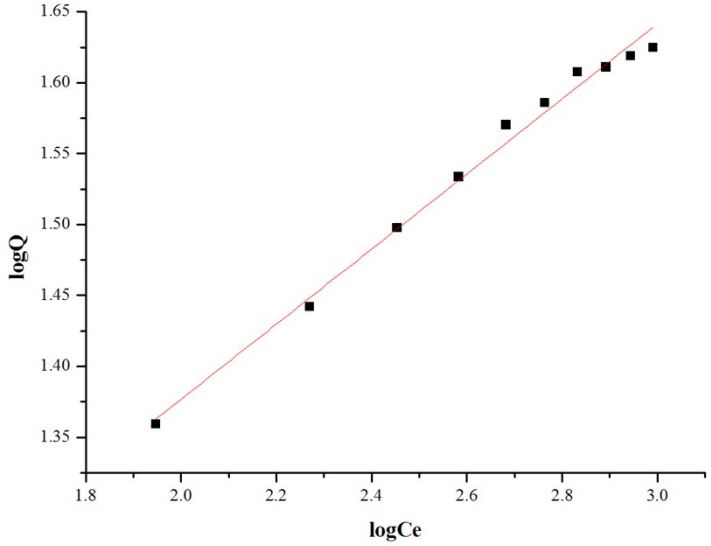

130

131 **Fig. S1-12** Fitting of the adsorption isotherm of CytC on the Fe_3O_4@ZIF-8 by using the Freundlich

132 model.

133

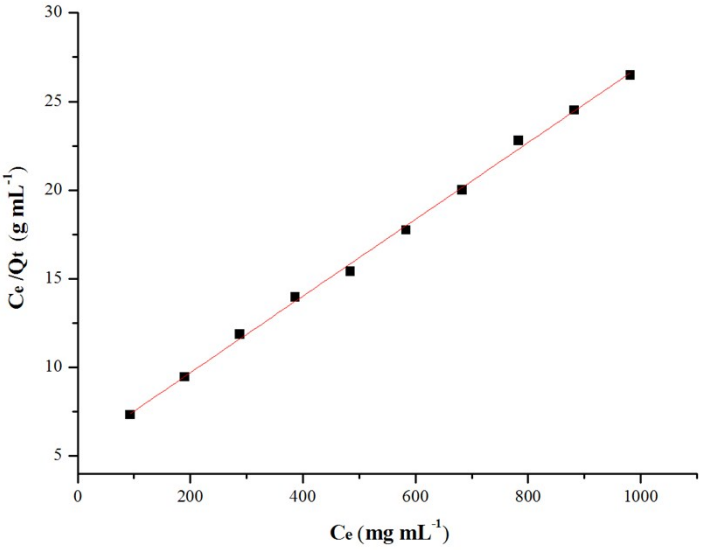

134

135 **Fig. S1-13** Fitting of the adsorption isotherm of HRP on the Fe_3O_4@ZIF-8 by using the Langmuir

136 model.

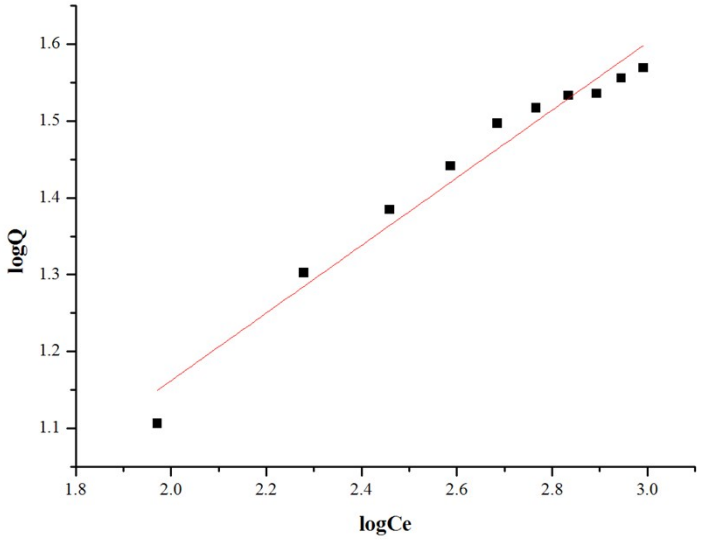

137

138 **Fig. S1-14** Fitting of the adsorption isotherm of HRP on the Fe_3O_4@ZIF-8 by using the Freundlich

139 model.

Table S2. Identification of proteins from digested human blood and the captured proteins by Fe_3O_4@ZIF-8.

Database Accession	Protein Name	Digested Human Blood			Captured Proteins by Fe_3O_4@ZIF-8		
		Distinct Peptides	% AA Coverage	Mean Peptide Spectral Intensity	Distinct Peptides	% AA Coverage	Mean Peptide Spectral Intensity
P68871	Hemoglobin subunit beta	11	80	3.49e+006	8	62	3.64e+006
P02042	Hemoglobin subunit delta	9	70	2.41e+006	8	61	2.94e+006
P69905	Hemoglobin subunit alpha	9	78	3.19e+006	8	59	3.07e+006
P02768	Serum albumin precursor	39	68	6.02e+005	13	24	1.35e+005
P01857	Ig gamma-1 chain C region	8	26	2.63e+005	5	19	9.10e+004
P01859	Ig gamma-2 chain C region	6	17	3.17e+005	4	13	1.35e+005
P01861	Ig gamma-4 chain C region	5	14	3.21e+005	3	11	1.36e+005
P01860	Ig gamma-3 chain C region	4	10	2.51e+005	2	6	7.81e+004
P01842	Ig lambda chain C regions	3	42	1.23e+005	2	23	6.06e+004
P01834	Ig kappa chain C region	3	50	2.18e+005	2	34	9.67e+004
P00915	Carbonic anhydrase 1	5	18	1.61e+005	/	/	/
P02647	Apolipoprotein A-I precursor	4	18	1.01e+005	6	26	1.44e+005
P01009	Alpha-1-antitrypsin precursor	4	9	1.04e+005	/	/	/
P32119	Peroxiredoxin-2	3	15	8.09e+004	/	/	/
Q06830	Peroxiredoxin-1	1	5	1.10e+005	/	/	/
P01023	Alpha-2-macroglobulin precursor	3	1	4.24e+004	2	1	2.47e+004
P00738	Haptoglobin precursor	3	6	7.96e+004	/	/	/
P00739	Haptoglobin-related protein precursor	2	4	8.67e+004	/	/	/
P02787	Serotransferrin precursor	2	3	5.37e+004	/	/	/
P01876	Ig alpha-1 chain C region	2	5	5.48e+004	/	/	/
P01877	Ig alpha-2 chain C region	1	2	7.56e+004	/	/	/

References

1. R. Fraczkiewicz and W. Braun, *J. Comput. Chem.*, 1998, **19**, 319–333.

2. H. M. Berman, J. Westbrook, Z. Feng, G. Gilliland, T. N. Bhat, H. Weissig, I. N. Shindyalov, and P. E. Bourne, *Nucleic Acids Res.*, 2000, **28**, 235–242.

3. S. A. Kuby, *A study of enzymes*, CRC Press, 1990, vol. 2.